

Supporting Information for

Strong influence of convective heat transfer efficiency on the cooling benefits of green roof irrigation

Linying Wang¹, Maoyi Huang^{2,3}, and Dan Li^{1*}

¹ Department of Earth and Environment, Boston University, Boston, MA 02215, United States of America

² Atmospheric Sciences and Global Change Division, Pacific Northwest National Laboratory, P.O. Box 999, Richland, WA 99352, United States of America

³ Now at Office of Science and Technology Integration, National Weather Service, National Oceanic and Atmospheric Administration, Silver Spring, MD 20910, United States of America

* Author to whom any correspondence should be addressed.

E-mail: lidan@bu.edu

Contents of this file

Text S1

Text S2

Figures S1 to S15

Tables S1 to S4

Introduction

This supporting information contains the descriptions of the stomatal resistance parameterization employed in the green roof module in CESM and the surface energy balance (SEB) model. It also provides results on the cooling effects of non-irrigated and well-irrigated green roofs for JJA and DJF seasons from land-only simulations (figures S1-S13), and results from the land-atmosphere coupled simulations (figures S14 and S15). The model parameters in the green roof parameterization are presented in tables S1-S2, and the model experiments are listed in table S3. The statistical results from the land-atmosphere coupled simulations are shown in table S4.

Text S1. The stomatal resistance parameterization

In the green roof module, we parameterize the impact of vegetation on ET through the stomatal resistance concept following Wang *et al* (2013):

$$ET = \frac{\rho(q_s^*(T_s) - q_a)}{r_a + r_s} \quad (S1)$$

where ρ (unit: kg m^{-3}) is the air density, $q_s^*(T_s)$ (kg kg^{-1}) is the saturated specific humidity at the surface temperature, q_a (kg kg^{-1}) is the air specific humidity, r_a (s m^{-1}) is the aerodynamic resistance, and r_s (s m^{-1}) is the stomatal resistance of vegetation parameterized using the so-called Jarvis scheme (Jarvis *et al* 1976). In this study, we follow the implementation by van Heerwaarden *et al* (2010) and van Heerwaarden and Teuling (2014):

$$r_s = \frac{r_{s,min}}{LAI} f_1(S_{in}) f_2(\theta) f_3(VPD) f_4(T_a) \quad (S2)$$

where $r_{s,min}$ is the minimal stomatal resistance (s m^{-1}), LAI is the leaf area index, and f_n are dimensionless stress functions dependent on the incoming shortwave radiation (S_{in} , W m^{-2}), the soil water content (θ , $\text{m}^3 \text{m}^{-3}$), the vapour pressure deficit (VPD , hPa), and the air temperature (T_a , K), as follows:

$$\frac{1}{f_1(S_{in})} = \min\left(1, \frac{0.004S_{in} + 0.05}{0.081(0.004S_{in} + 1)}\right) \quad (S3)$$

$$f_2(\theta) = \begin{cases} 0, & \theta < \theta_{wilt} \\ \frac{\theta - \theta_{wilt}}{\theta_{fc} - \theta_{wilt}}, & \theta_{wilt} \leq \theta \leq \theta_{fc} \\ 1, & \theta > \theta_{fc} \end{cases} \quad (S4)$$

$$\frac{1}{f_3(VPD)} = \exp(-g_D VPD) \quad (S5)$$

$$\frac{1}{f_4(T_a)} = 1.0 - 0.0016(298.0 - T_a)^2 \quad (\text{S6})$$

where θ_{wilt} and θ_{fc} are the soil water content at wilting point and field capacity, respectively; θ is the averaged soil water content over the entire green roof soil substrate; and g_D (hPa^{-1}) is an empirical coefficient that determines the strength of vegetation response to VPD . In the above stress functions, the first three are taken from the European Centre for Medium-Range Weather Forecasts (ECMWF) Integrated Forecasting System (IFS) and the fourth is taken from Noilhan and Planton (1989).

Text S2. A simple surface energy balance (SEB) model

The SEB model starts with the surface energy balance equation for an infinitely thin layer of a green roof, as follows:

$$R_n = S_{in}(1 - \alpha) + \varepsilon L_{in} - L_{out} = H + LE + G \quad (S7)$$

where R_n (W m^{-2}) is the net radiation; S_{in} (W m^{-2}) and L_{in} (W m^{-2}) are the incoming shortwave and longwave radiation, respectively; α and ε are the green roof albedo and emissivity, respectively; $L_{out} = \varepsilon\sigma T_s^4$ is the outgoing longwave radiation (W m^{-2}) where σ is the Stefan-Boltzmann constant ($\text{W m}^{-2} \text{K}^{-4}$) and T_s is the green roof surface temperature (K); H (W m^{-2}) and LE (W m^{-2}) are the sensible and latent heat fluxes, respectively; G is the heat flux (W m^{-2}) into the soil and the roof deck. Following convention, G is called the ground heat flux. The above equation can be reorganized as follows:

$$S_{in}(1 - \alpha) + \varepsilon L_{in} - LE = H + G + \varepsilon\sigma T_s^4 \quad (S8)$$

In doing so, we recognize that each term on the right-hand side of Eq. S8 is a function of surface temperature. Specifically, connecting H with surface temperature through the aerodynamic resistance concept, which measures the efficiency with which the green roof convects sensible heat into the urban air or the convective heat transfer efficiency (Garratt 1992), gives:

$$H = \frac{\rho c_p (T_s - T_a)}{r_a} \quad (S9)$$

where c_p ($\text{J kg}^{-1} \text{K}^{-1}$) is the specific heat of air at constant pressure, T_a (K) is the air temperature. The connection between G and surface temperature is achieved by using the force-restore method (Dickinson 1988), which describes that the evolution of the surface temperature can be expressed as the sum of a forcing term (related to G) and a restoring term,

$$\frac{dT_s}{dt} = \frac{\sqrt{2\omega}}{\mu} G - \omega(T_s - \bar{T}) \quad (\text{S10})$$

where μ is the thermal admittance ($\text{J m}^{-2} \text{K}^{-1} \text{s}^{-1/2}$), which is further determined by the volumetric heat capacity (c , $\text{J m}^{-3} \text{K}^{-1}$) and the thermal conductivity (λ , $\text{W m}^{-1} \text{K}^{-1}$) through $\mu = \sqrt{c\lambda}$, ω (s^{-1}) is the principal diurnal frequency, and \bar{T} (K) is the deep ground temperature (in our case \bar{T} can be viewed as the temperature of the building interior).

Substituting Eqs. S9-S10 into S8 yields

$$\frac{dT_s}{dt} = \frac{\sqrt{2\omega}}{\mu} \left[S_{in}(1 - \alpha) + \varepsilon L_{in} - \varepsilon \sigma T_s^4 - \frac{\rho C_p (T_s - T_a)}{r_a} - LE \right] - \omega(T_s - \bar{T}) \quad (\text{S11})$$

To proceed, we linearize the outgoing longwave radiation at air temperature and simplify the equation as:

$$\frac{dT_s}{d\tau} = -\frac{T_s}{f} + Q' \quad (\text{S12})$$

where τ is a new time scale of the unit $\text{K W}^{-1} \text{m}^2$, Q' is a forcing term (W m^{-2}), and f is a surface energy redistribution factor ($\text{K W}^{-1} \text{m}^2$) that encodes the efficiencies of different surface energy balance components in transferring heat:

$$\tau = \frac{t}{\mu/\sqrt{2\omega}} \quad (\text{S13})$$

$$Q' = S_{in}(1 - \alpha) + \varepsilon L_{in} + 3\varepsilon \sigma T_a^4 + \frac{\rho C_p}{r_a} T_a + \mu \sqrt{\frac{\omega}{2}} \bar{T} - LE \quad (\text{S14})$$

$$f = \frac{1}{\frac{1}{r_a} + \frac{1}{r_g} + \frac{1}{r_o}} \quad (\text{S15})$$

$$r_a' = \frac{r_a}{\rho c_p} \quad (\text{S16})$$

$$r_g' = \frac{1}{\mu \sqrt{\frac{\omega}{2}}} \quad (\text{S17})$$

$$r_o' = \frac{1}{4\varepsilon\sigma T_a^3} \quad (\text{S18})$$

The $1/r_a'$, $1/r_g'$, and $1/r_o'$ in f represent the linearized heat transfer efficiencies ($\text{W m}^{-2} \text{K}^{-1}$) for convection, conduction (in this case conduction means heat transfer into the soil and the roof deck), and radiation, respectively. These efficiencies link changes in the respective heat fluxes with changes in the surface temperature. Physically, the convection efficiency represents the effect of atmospheric turbulence in transferring sensible heat and thus depends on the turbulent intensity, which further depends on the wind shear and atmospheric stability (Garratt 1992). The conduction efficiency represents the effect of thermal admittance in determining heat conduction in the soil and the roof deck (Oke *et al* 2017). These efficiencies may be interpreted as climate feedback parameters at local scales, considering that the radiation efficiency simply represents the strength of Planck feedback (Bony *et al* 2006). In our study, the magnitude of these efficiencies indicates the tendency of the surface to alter these heat fluxes when a perturbation occurs: a larger efficiency means a stronger tendency for the heat flux to respond to perturbations. The solution for Eq. S12 is

$$T_s = T_s(0)e^{-\tau/f} + Q'f \quad (\text{S19})$$

where $T_s(0)$ is the initial condition for the green roof surface temperature (K).

The key difference between our derivation here and previous work is that we do not treat LE as a function of surface temperature (i.e., not a response variable) because we want to link it to irrigation. Specifically, we assume that the difference in LE (or ΔLE) between an

irrigated and a non-irrigated green roof is equal to the irrigation water amount ($Q_{irrigation}$, $\text{kg m}^{-2} \text{s}^{-1}$ or mm s^{-1}) multiplied by the latent heat of vaporization (L_v , J kg^{-1}), which is a very weak function of temperature and is treated as a constant in our study ($= 2.5 \times 10^6 \text{ J kg}^{-1}$). This effectively assumes that all irrigated water evaporates (i.e., the changes in runoff or storage induced by irrigation are negligible). If we further assume that green roof irrigation does not affect other atmospheric forcings such as incoming radiation and also green roof surface properties such as surface albedo and emissivity, then we can express the surface temperature difference between an irrigated and a non-irrigated green roof under steady-state conditions as

$$(\Delta T_s)_{SEB} = \Delta Q' f = -\Delta L E f = -L_v Q_{irrigation} f \quad (\text{S20})$$

This is the final result of the SEB model.

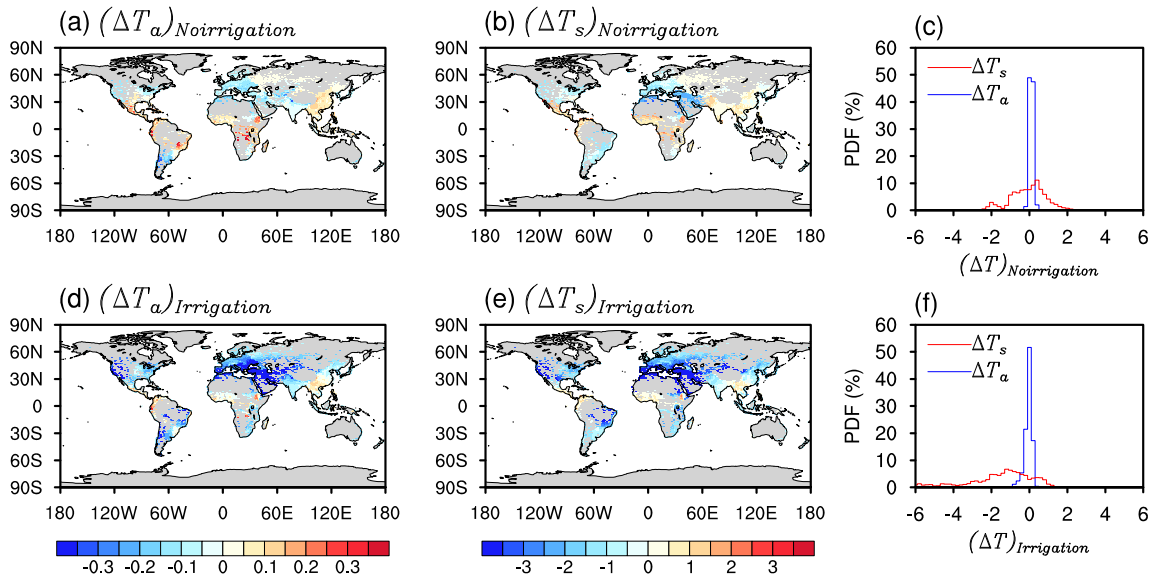


Figure S1. Similar to figure 2 but for JJA.

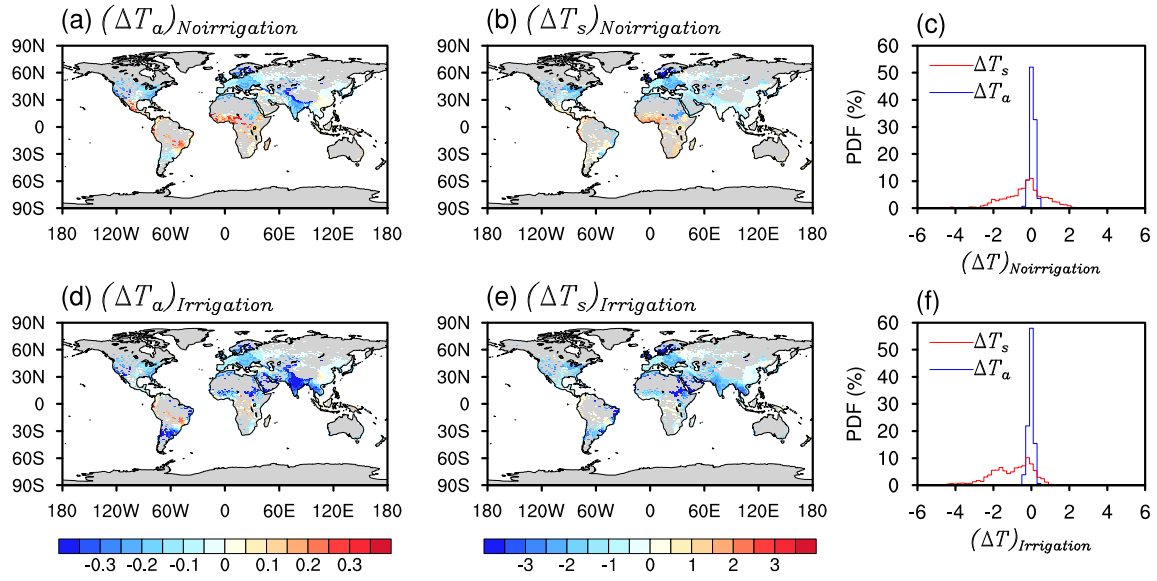


Figure S2. Similar to figure 2 but for DJF.

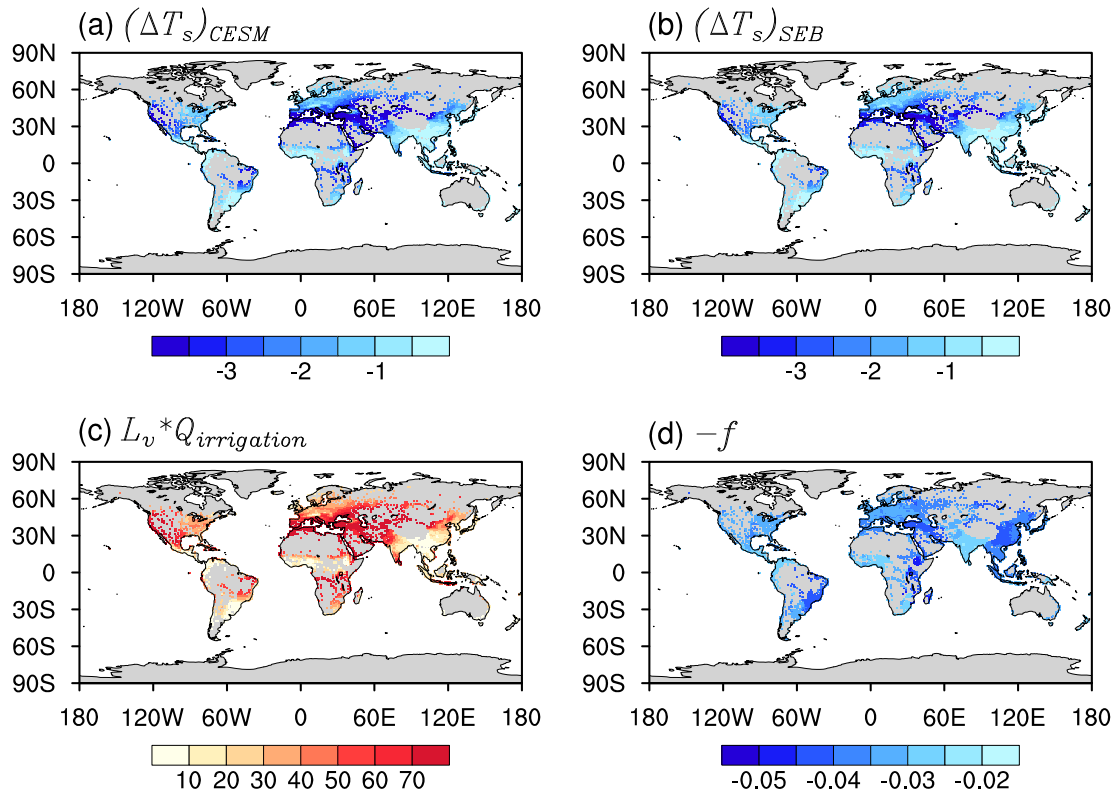


Figure S3. Similar to figure 3 but for JJA.

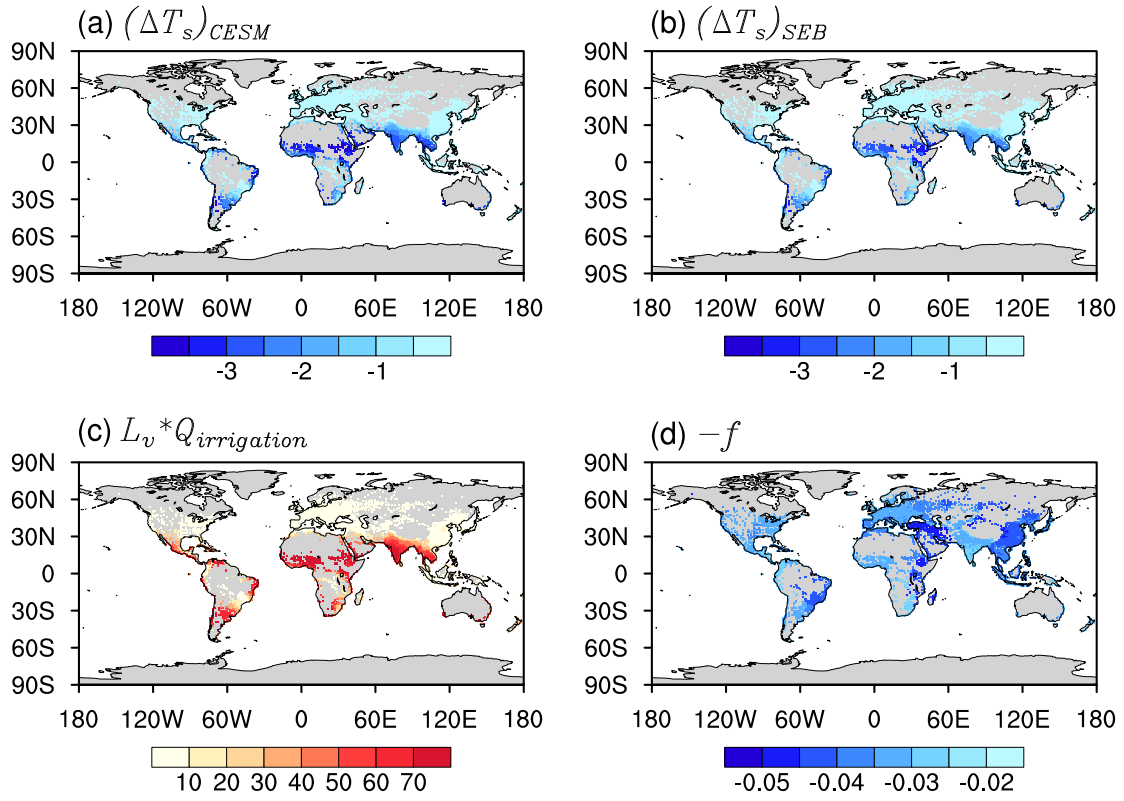


Figure S4. Similar to figure 3 but for DJF.

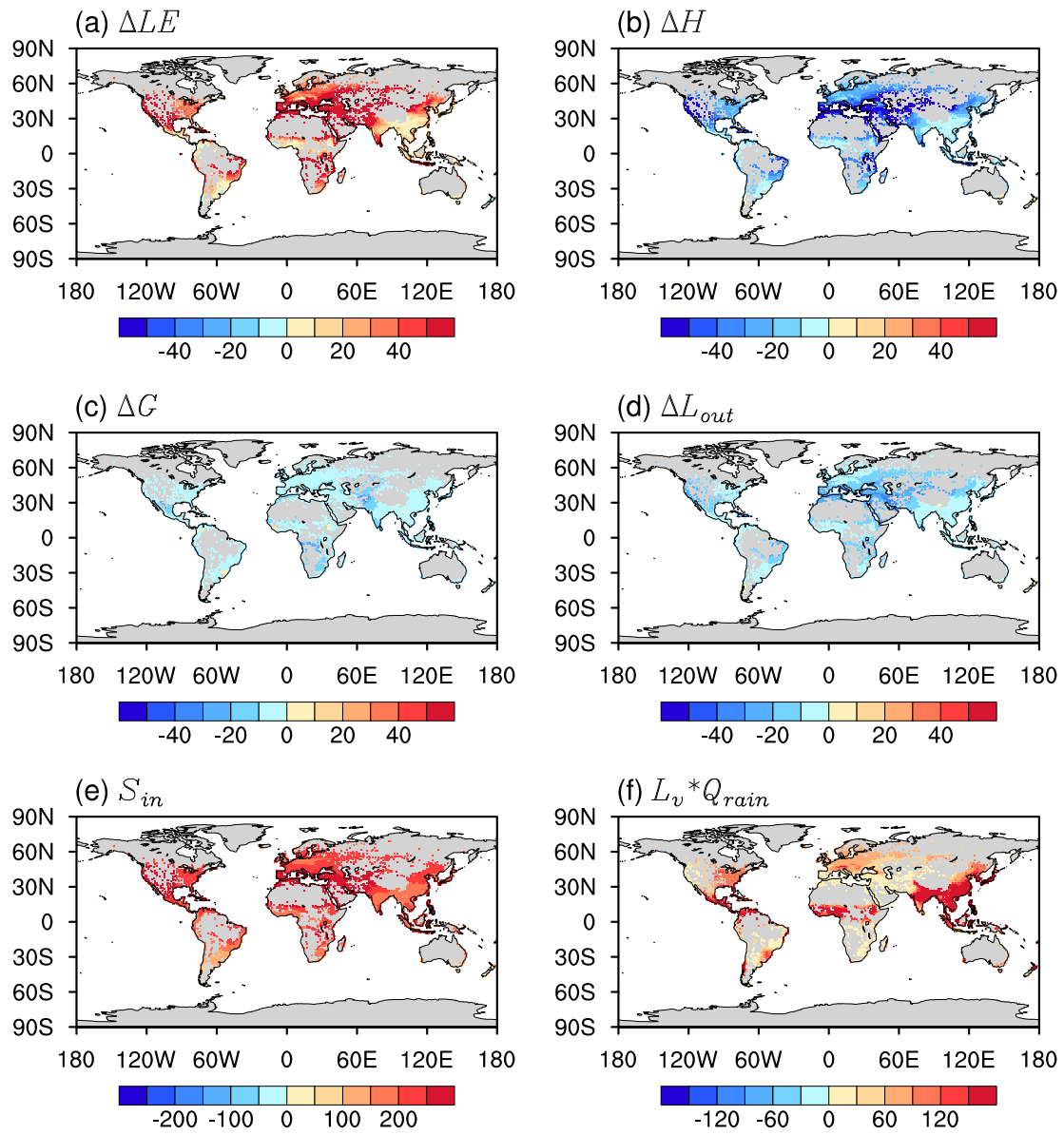


Figure S5. Similar to figure 4 but for JJA.

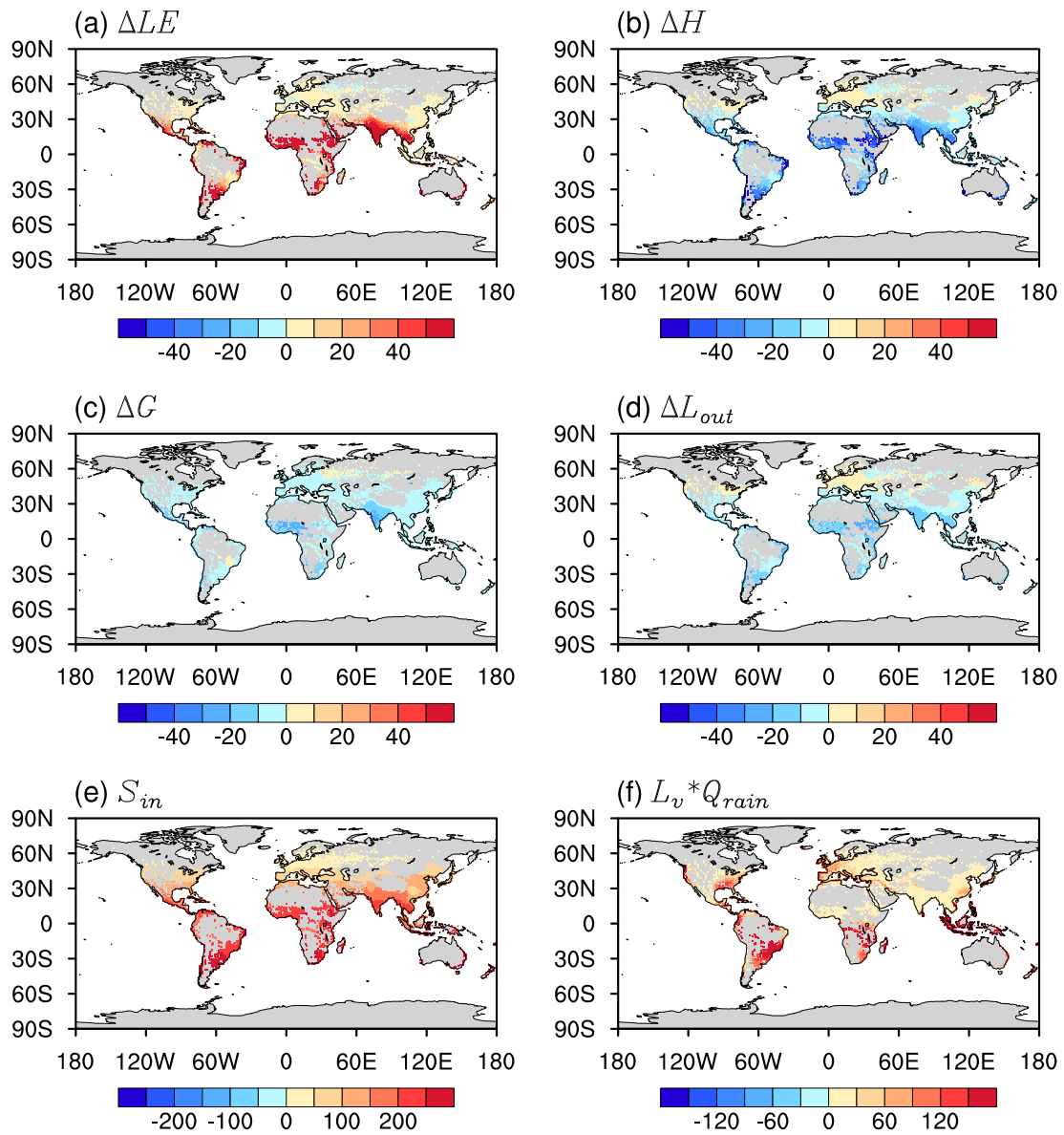


Figure S6. Similar to figure 4 but for DJF.

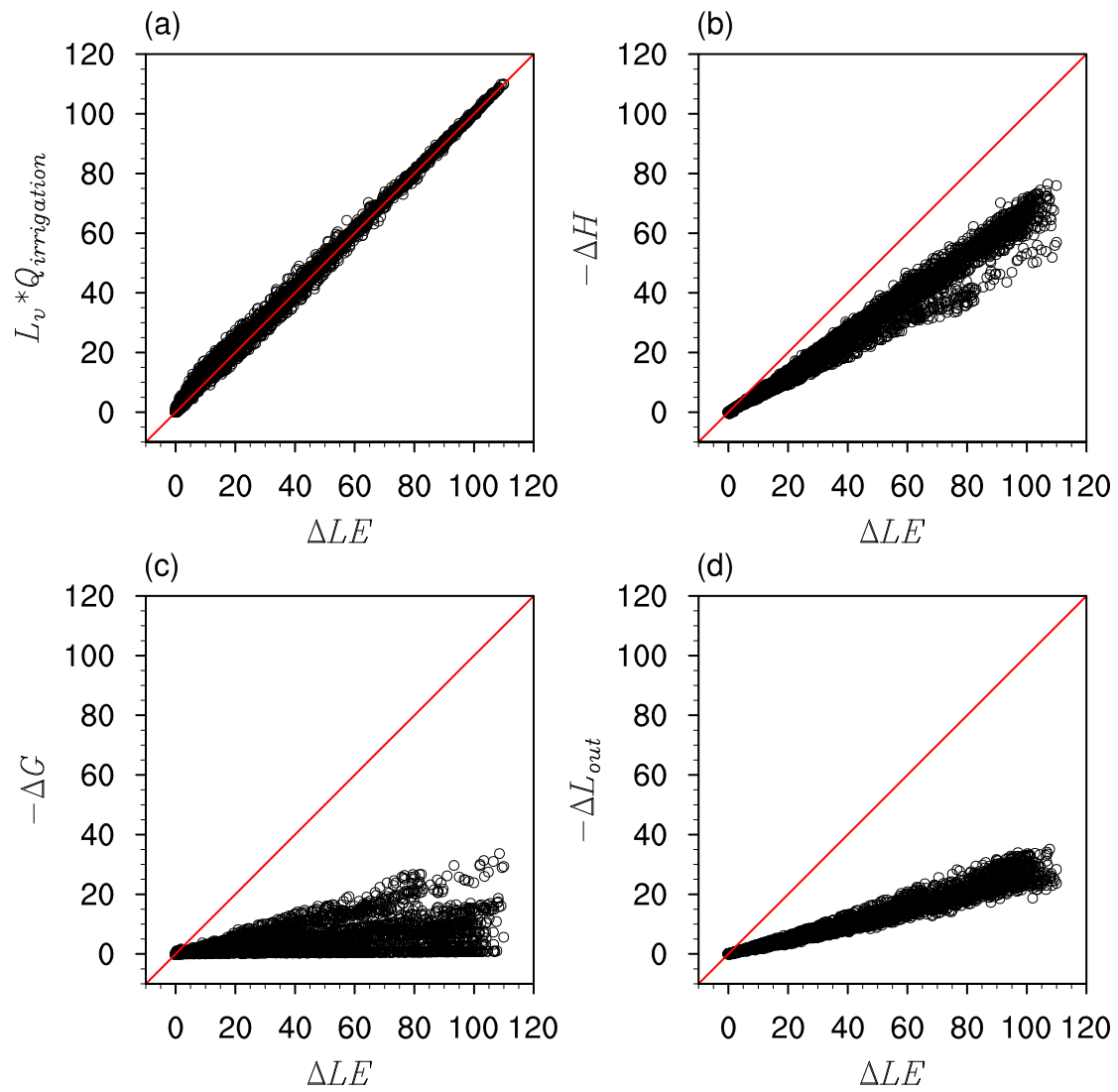


Figure S7. Similar to figure 5 but for JJA.

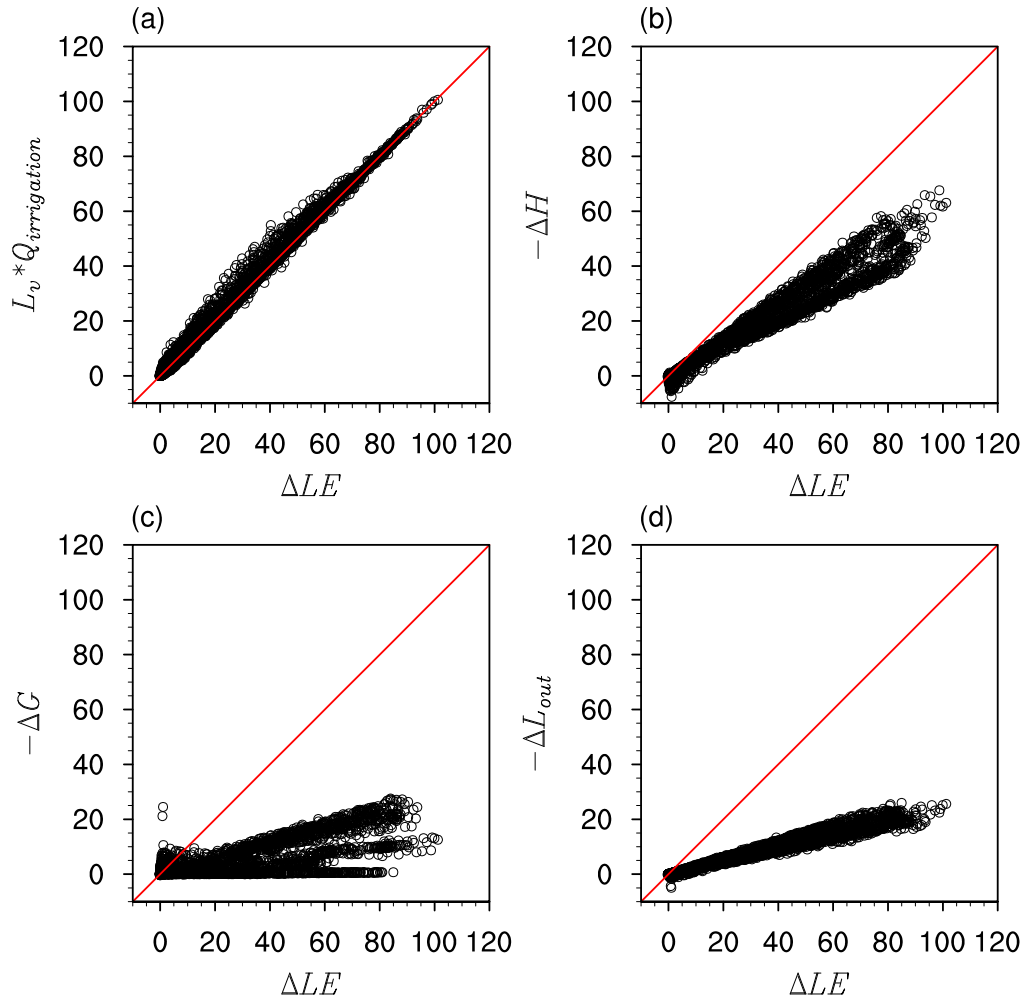


Figure S8. Similar to figure 5 but for DJF.

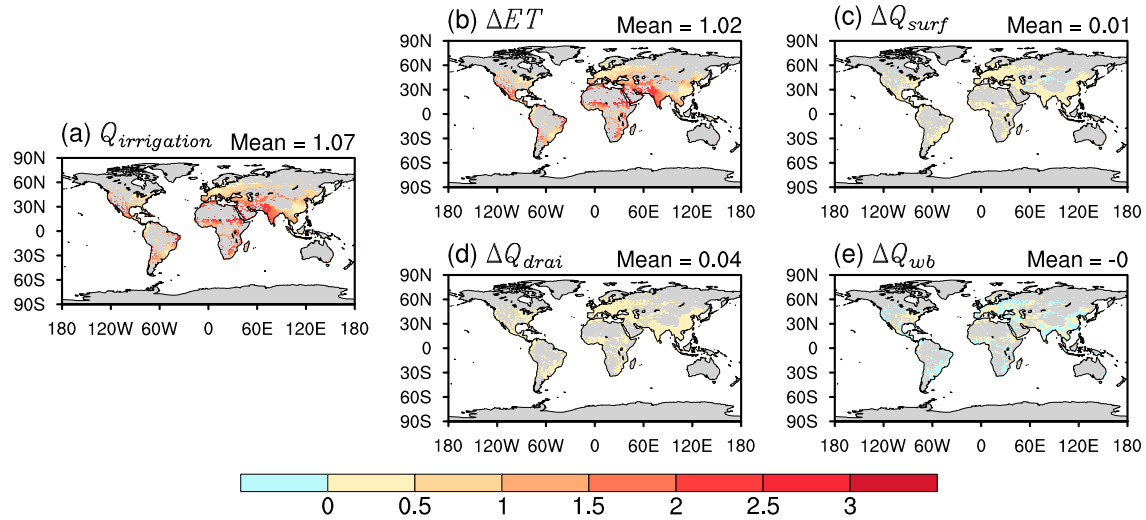


Figure S9. The green roof annual mean (a) irrigation water amount ($Q_{irrigation}$) simulated by the Case_Irrigation, and its induced changes in (b) evapotranspiration (ΔET), (c) surface runoff (ΔQ_{surf}), (d) sub-surface drainage (ΔQ_{drai}), and (e) changes of soil water storage (ΔQ_{wb}). Also shown are the global averaged values for the corresponding variables in each sub-figure. All units are mm day^{-1} . The results are the annual daily mean over 20 years (1991-2010) from land-only simulations. Only grid cells with more than 0.1% of urban land are shown and calculated for the global averages.

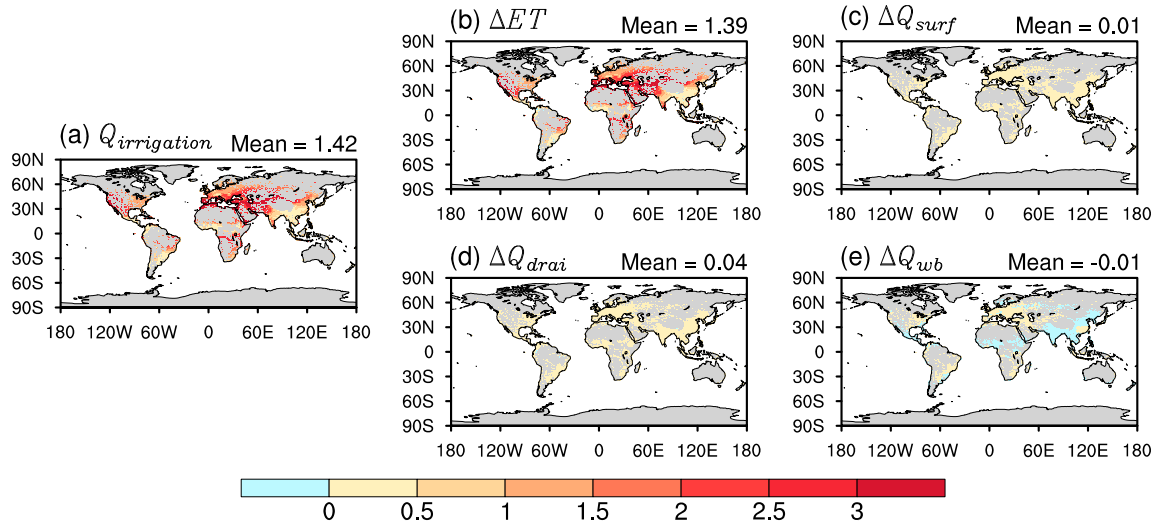


Figure S10. Similar to figure S9 but for JJA.

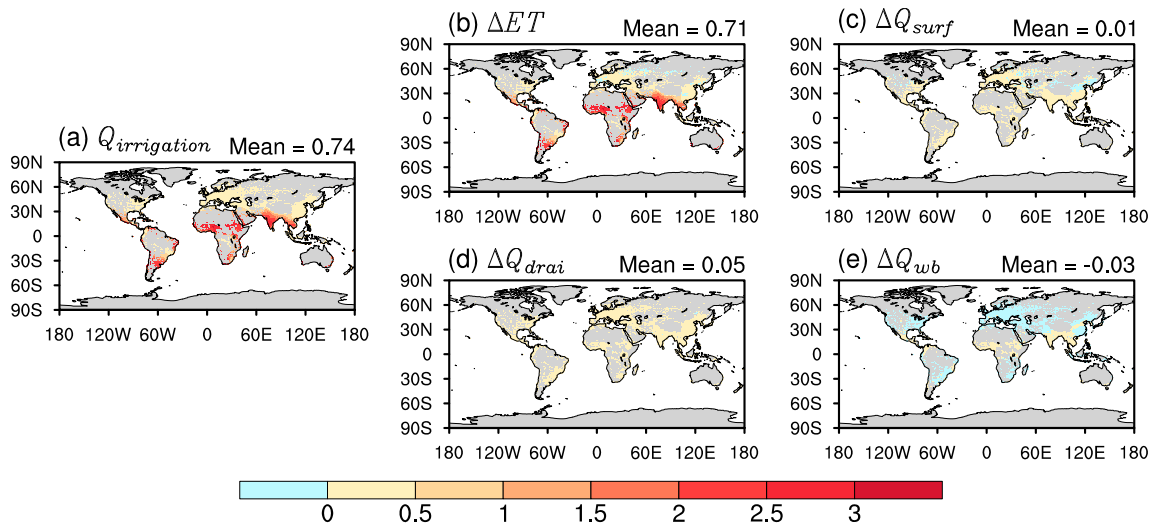


Figure S11. Similar to figure S9 but for DJF.

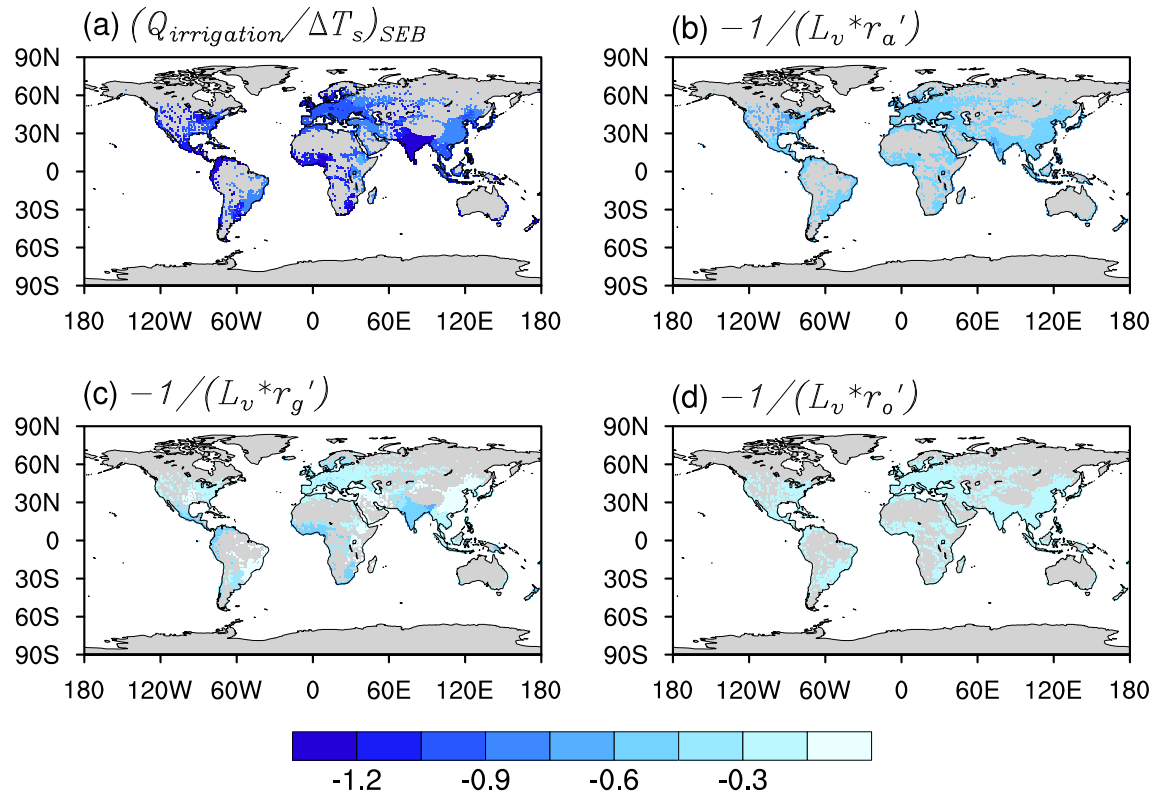


Figure S12. Similar to figure 6 but for JJA.

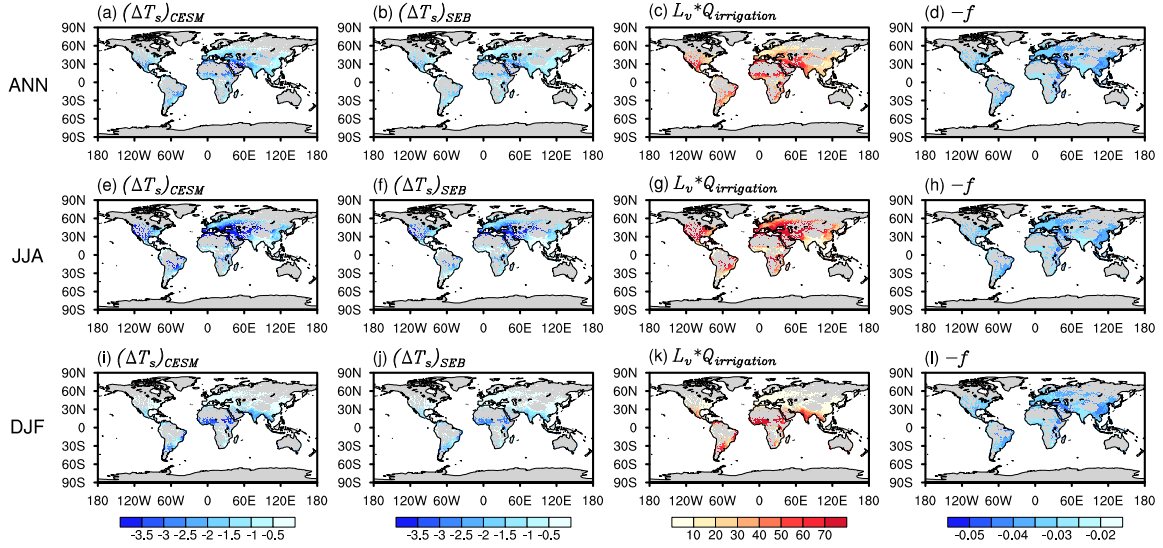


Figure S14. Surface temperature reduction due to green roof irrigation (unit: K) simulated by (a) CESM and predicted by (b) SEB. Also shown are the (c) irrigation water amount multiplied by the latent heat of vaporization (unit: W m^{-2}) and (d) surface energy redistribution factor f (unit: $\text{K W}^{-1} \text{m}^2$). The irrigation water amount is from the Case_Irrigation output and the surface energy redistribution factor f is calculated based on Eq. S15-S18 using the Case_Noirrigation outputs. (a-d) are the annual daily mean (ANN), (e-h) are the JJA daily mean, and (i-l) are the DJF daily mean results from land-atmosphere coupled simulations over 20 years (1991-2010). Only grid cells with more than 0.1% of urban land are shown.

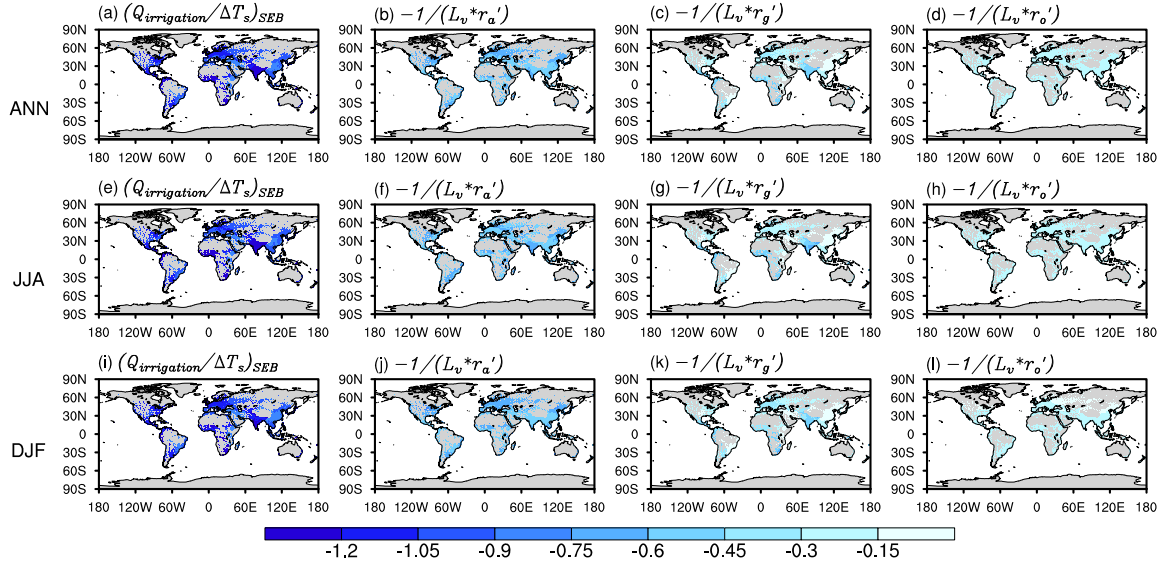


Figure S15. The SEB predicted (a) irrigation water demand per unit decrease of surface temperature for green roofs, and the individual contributions from the (b) convection, (c) conduction, and (d) radiation efficiencies. All units are $\text{mm day}^{-1} \text{K}^{-1}$. (a-d) are the annual daily mean (ANN), (e-h) are the JJA daily mean, and (i-l) are the DJF daily mean results from land-atmosphere coupled simulations over 20 years (1991-2010). Only grid cells with more than 0.1% of urban land are shown.

Table S1. Model parameters used in the green roof parameterization for global runs.

Variable	Description and unit	Value
α	albedo (-)	0.3 (Sun <i>et al</i> 2013)
ε	emissivity (-)	0.95 (Sun <i>et al</i> 2013)
$R_{s,min}/LAI$	minimum stomatal resistance / leaf area index ($s\ m^{-1}$)	180/3 (van Heerwaarden and Teuling 2014)
$R_{s,max}$	maximum stomatal resistance ($s\ m^{-1}$)	5000 (Wang <i>et al</i> 2013)
g_D	exponent for VPD response (hPa^{-1})	0.03
f_{max}	maximum fractional saturated area (-)	0.72
β	topographic slope (degree)	0.2
d	soil depth (m)	0.2
%sand	percent sand (%)	41 (Tian <i>et al</i> 2017)
%clay	percent clay (%)	22 (Tian <i>et al</i> 2017)

Table S2. Green roof model parameters specific for the experimental site on the campus of Tsinghua University, Beijing, China. The parameters are obtained from Sun *et al* (2013).

Variable	Description and unit	Value
c	volumetric heat capacity of vegetation-soil, medium and concrete layers ($\text{MJ m}^{-3} \text{K}^{-1}$)	1.6, 2.0, 2.9
λ	thermal conductivity of vegetation-soil, medium and concrete layers ($\text{W m}^{-1} \text{K}^{-1}$)	0.8, 1.2, 1.8
θ_{sat}	saturated soil water content ($\text{m}^3 \text{m}^{-3}$)	0.36
θ_{fc}	soil water content at field capacity ($\text{m}^3 \text{m}^{-3}$)	0.31
θ_{wilt}	soil water content at wilting point ($\text{m}^3 \text{m}^{-3}$)	0.18
B	fitting exponent for unsaturated soil (-)	2.33
ψ_{sat}	saturated soil matric potential (mm)	500
k_{sat}	saturated hydraulic conductivity (mm s^{-1})	0.117

Table S3. A list of simulations performed in this study.

	Case names	Regular roof fraction	Green roof fraction	Irrigation
Land-only simulations	CTL	100%	0	No
	Case_Noirrigation	0	100%	No
	Case_Irrigation	0	100%	Yes
Land-atmosphere coupled simulations	Case_Noirrigation_LA	0	100%	No
	Case_Irrigation_LA	0	100%	Yes

Table S4. Similar to table 1 but for land-atmosphere coupled simulations.

R^2	ANN	JJA	DJF
$(\Delta T_s)_{CESM}$ and $(\Delta T_s)_{SEB}$	0.96	0.96	0.92
$(\Delta T_s)_{CESM}$ and $(L_v * Q_{irrigation})$	0.90	0.93	0.90
$(\Delta T_s)_{CESM}$ and f	0.04	0.15	0.00

References

- Bony S *et al* 2006 How well do we understand and evaluate climate change feedback processes? *J. Clim.* **19** 3445-3482 doi: 10.1175/JCLI3819.1
- Dickinson R E 1988 The force-restore model for surface temperatures and its generalizations *J. Clim.* **1** 1086-1097 doi: 10.1175/1520-0442(1988)001<1086:Tfmfst>2.0.Co;2
- Garratt J R 1992 *The atmospheric boundary layer* (Cambridge: Cambridge University Press)
- Jarvis P G, Monteith J L and Weatherley P E 1976 The interpretation of the variations in leaf water potential and stomatal conductance found in canopies in the field *Philos. Trans. R. Soc. Lond. B.* **273** 593-610 doi: 10.1098/rstb.1976.0035
- Noilhan J and Planton S 1989 A simple parameterization of land surface processes for meteorological models *Mon. Weather Rev.* **117** 536-549 doi: 10.1175/1520-0493(1989)117<0536:ASPOLS>2.0.CO;2
- Oke T R, Mills G, Christen A and Voogt J A 2017 *Urban climates* (Cambridge: Cambridge University Press)
- Sun T, Bou-Zeid E, Wang Z-H, Zerba E and Ni G-H 2013 Hydrometeorological determinants of green roof performance via a vertically-resolved model for heat and water transport *Build. Environ.* **60** 211-224 doi: 10.1016/j.buildenv.2012.10.018

- Tian Y, Bai X, Qi B and Sun L 2017 Study on heat fluxes of green roofs based on an improved heat and mass transfer model *Energy Build.* **152** 175-184 doi: 10.1016/j.enbuild.2017.07.021
- van Heerwaarden C C and Teuling A J 2014 Disentangling the response of forest and grassland energy exchange to heatwaves under idealized land-atmosphere coupling *Biogeosciences* **11** 6159-6171 doi: 10.5194/bg-11-6159-2014
- van Heerwaarden C C, Vilà-Guerau de Arellano J, Gounou A, Guichard F and Couvreux F 2010 Understanding the daily cycle of evapotranspiration: A method to quantify the influence of forcings and feedbacks *J. Hydrometeorol.* **11** 1405-1422 doi: 10.1175/2010JHM1272.1
- Wang Z-H, Bou-Zeid E and Smith J A 2013 A coupled energy transport and hydrological model for urban canopies evaluated using a wireless sensor network *Q. J. R. Meteorol. Soc.* **139** 1643-1657 doi: 10.1002/qj.2032